Precipitation of $(Pd_xAg_{1-x})_3$ In in Ag-25% Pd-In alloys and the partial phase diagram of ternary Ag-Pd-In alloys

YONG CHAN SUH, ZIN HYOUNG LEE
Department of Materials Science and Engineering, Korea Advanced Institute of Science and Technology, 373-1 Kusung-Dong, Yusung-Gu, Taejon, 305-701, Republic of Korea
E-mail: s_syc@cais.kaist.ac.kr

MICHIO OHTA
Department of Dental Materials Engineering, Faculty of Dentistry, Kyushu University, 3-1-1 Maedashi, Higashi-ku, Fukuoka 812-82, Japan

A study was carried out to determine the partial phase diagram for the system Ag-25 wt % Pd–y wt% In with $y \leq 8$ by X-ray powder diffraction and differential thermal analysis. The liquidus and solidus temperatures decreased with increasing indium content up to 8 wt % In for a given 25 wt % Pd. The solvus curve of γ phase identified as $(Pd_xAg_{1-x})_3$ In was determined by the parametric method and the temperature dependence of In-solubility in Ag-25 wt % Pd was very strong above 900 °C.

1. Introduction

The high price of gold dental alloys has created a demand for cheaper crown and bridge alloys, which has been met by manufacturers to the extent that a variety of alternative alloys are now available. These alternative alloys fall into three main categories: gold-reduced alloys; silver-palladium alloys and base metal alloys. The silver-palladium alloys have been widely used recently because of their low cost, reasonably good castability and corrosion properties. Another favorable feature of this type of alloy is its age-hardenability when elements such as Cu, Zn, Sn, Ga and In are added [1].

However, Ag-Pd-X has usually been used without much basic knowledge on phase diagram and precipitation behavior. Some work has been done to assess the ternary system Ag-Pd-Cu [2], but phase diagrams of other Ag-Pd-X ternary systems are still missing. In particular, the information on the Ag-Pd-In phase diagram is important, because In is added very often as an alloying element and proper heat treating conditions need to be established. Proper knowledge of the phase diagram may also provide a basis for better understanding of the mechanical behavior of the alloy.

In this paper, the precipitation behavior and the partial phase diagram of the ternary Ag-25 wt % Pd–y wt % In with up to 8 wt % In were investigated by differential thermal analysis, X-ray powder diffraction and microscopic observation.

2. Experimental procedures

The alloys were prepared from materials of purity higher than 99.99% in evacuated quartz ampullae by high frequency induction melting. The mass of each alloy was 8 g. Since the weight loss in the melting and alloying process was less than 0.1%, chemical analysis after melting was not carried out. The ingots were slightly cold-worked and homogenized at 980 °C for 2 h for the composition below 5% In and 1020 °C for 2 h for the composition above 6% In.

The liquidus and solidus temperatures of the alloys were determined by differential thermal analysis (DTA, Rigaku Co. Ltd). Solidus point was determined in the heating portion of the thermal cycle and liquidus point in the cooling portion. Heating and cooling rates of 5 °C/min were used.

X-ray diffraction (XRD) was carried out to determine the phase boundaries in the solid state. Powders that passed through a 330-mesh screen were produced using a rotating diamond grinding disk. These powders were sealed in an evacuated silica capsule. They were heat-treated for 1 h at the appropriate temperature and quenched directly into ice-brine. The powders were examined in an RINT-2500V standard-type diffractometer (Rigaku Co. Ltd). The X-ray source was a rotating anode copper target operating at 40 kV and 200 mA. Cu-Kα radiation was used as the incident beam. The parametric method [3] was used and lattice

parameters were determined by the least-squares method.

The specimens for microstructure examination were etched in a solution of 2.5% KCN and 2.5% $(NH_4)S_2O_8$ in water and examined in a Phillips scanning electron microscope (SEM).

3. Results and discussion

3.1. Differential thermal analysis

Fig. 1 shows a part of the typical DTA curve of 4% In alloy during the thermal cycle. The results of the liquidus and solidus temperature determination are also shown, together with the composition of the alloys, in Table I. Indium contents range from 2 to 8% in steps of approximately 1% for 25% palladium content and the solidification range of binary Ag-25% Pd alloy marked with an asterisk was obtained from the binary phase diagram [4]. In general, the melting point of pure component is readily obtained from the heating curve of DTA and can be sharply defined, while the melting point of the alloy is not sharply defined in particular, the liquidus temperature. Therefore, the cooling curve of DTA was used in order to determine the liquidus points of alloys [5] as shown in Fig. 1.

Table I shows a faster decrease in the solidus temperature than in the liquidus temperature with increasing indium content. From the continuous decrease of liquidus and solidus temperature and the peak shape of DTA curves, it may be concluded that no invariant reaction exists up to 8% In.

3.2. Determination of a solvus curve in the solid state

The solvus curve in the Ag-Pd-In ternary system was determined by the parametric method. Powders with different In-content were equilibrated at the same temperature and quenched directly into ice-brine. The lattice parameter of α phase (Ag-rich phase) was measured by XRD and plotted against the indium concentration as shown in Fig. 2. It was noted that the slope of each lattice parameter versus composition curve apparently changed at around 4% for 900 °C and around 5% for 980 °C. This indicates the phase boundary between the single-phase and two-phase region of the ternary system. This result also agrees with Fig. 3. That is, the first additions of indium to binary Ag-25% Pd go into a α–solid solution and the lattice parameter of α phase increases continuously with the indium concentration until a second phase begins to precipitate. α phase has a limited solubility because the atomic diameter of In (33.2 nm) is about 15% bigger than that of Ag (28.8 nm).

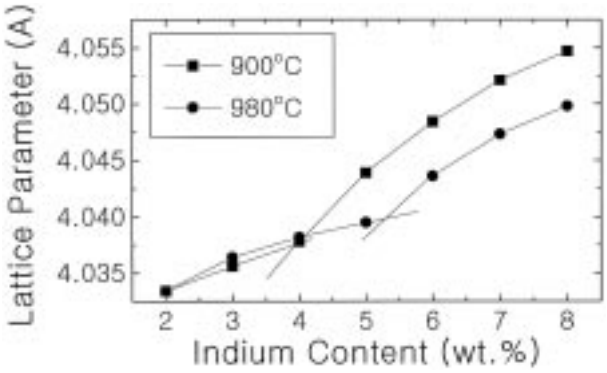

Figure 2 Lattice parameter versus composition at several temperatures for Ag-25% Pd-y% In alloys for 1 h.

When the solubility limit of indium in Ag-25% Pd is reached, the further additions of indium cause the precipitation of a second phase. This second phase γ has been identified as $(Pd_xAg_{1-x})_3In$ which has a tetragonal structure with $c/a = 1.24 \sim 1.25$ calculated with the result of Fig. 3. In the case of the binary Pd-In system, it is known that the c/a of Pd_3In [6] is $0.90 \sim 0.93$. The lattice parameter of the γ phase in the ternary Ag-Pd-In system is elongated more toward the c axis.

With increasing amount of precipitation the lattice parameter curve of α phase in the two-phase region has the higher slope than in the single phase region. It should be related to the solubility change of Pd and In in the α phase. The lattice parameter of the binary Ag-Pd alloy reported by Coles [7] showed a linear decrease with increasing palladium content due to the smaller atomic diameter of Pd (27.5 nm). It is considered that the lattice parameter of the α phase in the two-phase region increases because the Pd and In content in the α phase decrease with increasing amounts of precipitates.

Fig. 4 shows the microstructures of Ag-25% Pd with 2

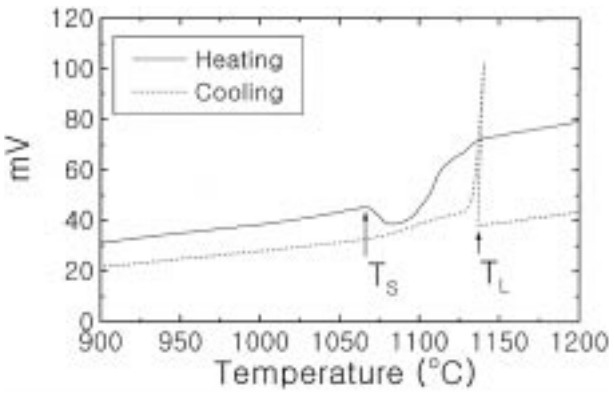

Figure 1 A typical DTA curve of Ag-25% Pd-4% In alloy.

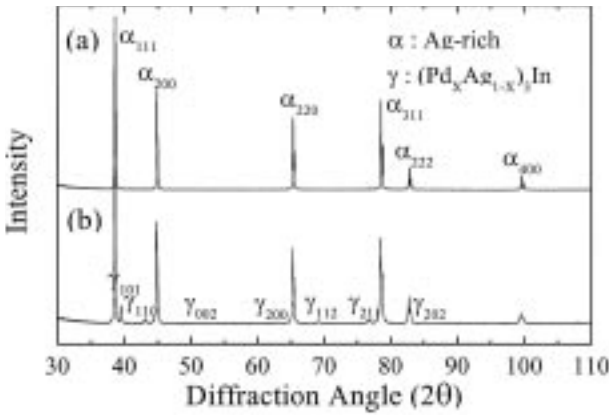

Figure 3 XRD patterns of (a) the Ag-25% Pd-3% In alloy and (b) the Ag-25% Pd-4% In alloy equilibrated at 900 °C for 1 h.

TABLE I Chemical composition and solidification range of alloys studied

Alloys	Composition (wt%)			Temperature (°C)	
	Ag	Pd	In	Liquidus (T_L)	Solidus (T_S)
0% In	75	25	—	*1179	*1136
2% In	73	25	2	1153	1095
3% In	72	25	3	—	—
4% In	71	25	4	1140	1067
5% In	70	25	5	1133	1054
6% In	69	25	6	1132	1042
7% In	68	25	7	1128	1033
8% In	67	25	8	1128	1025

to 8% In after annealing at 900 °C for 1 h. Fig. 4a shows the microstructure of 2% In with annealing twins [8]. No second phase has been observed anywhere, which implies a single phase α with a fcc structure is stable at 900 °C. The results agree well with the results of XRD Fig. 4b with 4% In, however, shows a second phase, mostly along the grain boundaries. The second phase was already identified as a $(Pd_xAg_{1-x})_3In$ phase by XRD as explained above. Fig. 4c with 6% In also shows a plate-like precipitate in the grain interior as well as grain boundaries. The microstructure of Fig. 4d with 8% In is similar to the that of 6% In, although the size of the plate-like precipitates seems to have grown somewhat. This is due to the higher In-content.

3.3. Phase diagram

On the basis of the XRD results, the resulting solvus curve is drawn in the Ag-25% Pd–*y*% In vertical section of the ternary phase diagram of Ag-Pd-In as shown in Fig. 5. The maximum solubilities of In in Ag and Pd are both about 21 wt% at 695 °C and 1357 °C, respectively [4]. The temperature dependence of In-solubility is larger in Ag-25% Pd–*y*% In than in both binary systems. Therefore these alloys can be considered as hardenable alloys such as Ag-Pd-Cu alloys, although the single phase temperature region is relatively narrow.

The resulting partial phase diagram for the ternary Ag-Pd-In system is deduced from the results of this work and the binary phase diagrams as shown in Fig. 6. No previous reports on this ternary phase diagram have been published, and thus a comparison with other results is not possible. Fig. 6 shows the suggested solvus surface, marked with a dashed line on the isothermal section of 800 °C. The continuation of this solvus surface toward the binary Ag-In system is uncertain because the γ phase of Ag-25% Pd–*y*% In has the same structure as in the Pd-In system but is different from the ζ phase which has a hexagonal structure in the binary Ag-In system [4].

4. Conclusion

By means of DTA, XRD and microstructure examination, the following results were obtained for the ternary Ag-25% Pd-*y*% In alloys. A partial phase diagram is

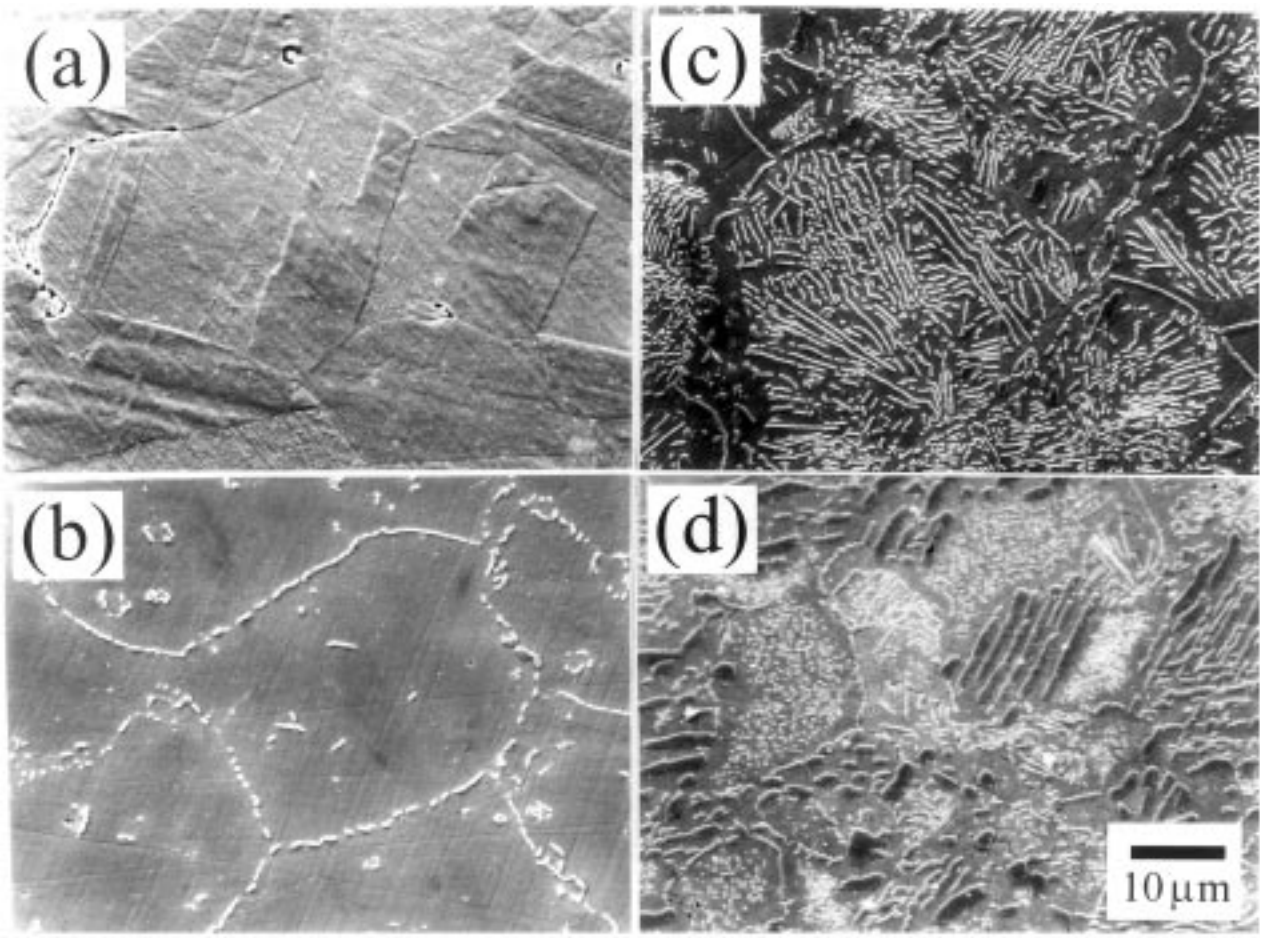

Figure 4 The SEM microstructures of (a) 2% In, (b) 4% In, (c) 6% In and (d) 8% In-Ag-25% Pd alloy heated at 900 °C for 1 hr.

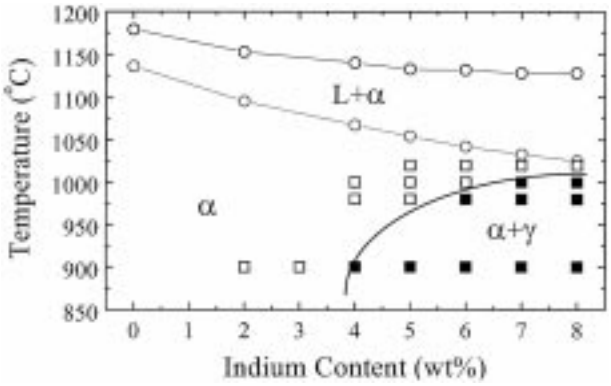

Figure 5 Partial phase diagram for the system Ag-25% Pd-*y*% In; ○, ● ; liguidus and solidus temperature measured from DTA, □, ■; single and two-phase region measured from XRD.

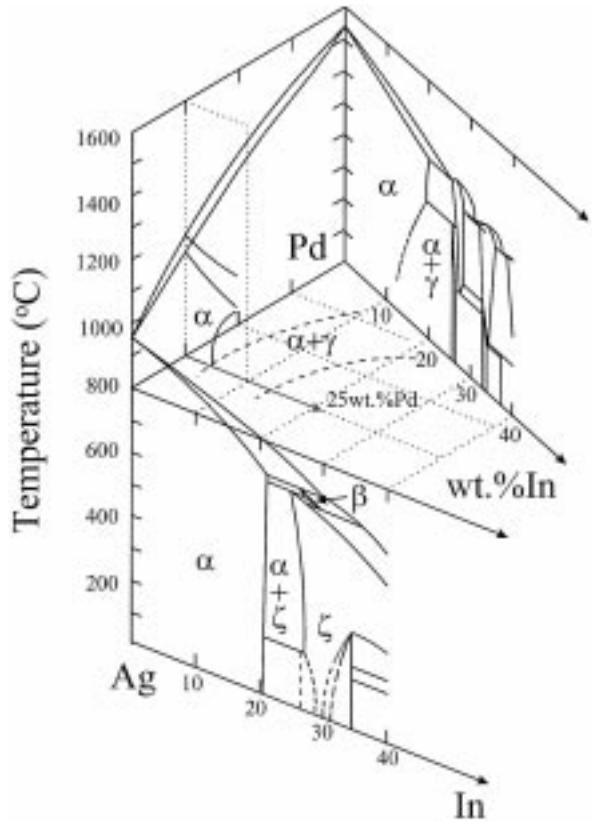

Figure 6 Phase diagrams of binary Ag-Pd, Pd-In and Ag-In and the isothermal section of ternary Ag-Pd-In at 800 °C.

constructed up to 8% indium content. Liquidus temperature and solidus temperature decrease with increasing indium content. The temperature dependence of In-solubility in Ag-25% Pd is very strong above 900 °C. The precipitating phase is $(Pd_xAg_{1-x})_3In$. It precipitates at 4% In mostly on grain boundaries and at higher In-content also inside grains.

Acknowledgments

The research was performed under financial support from KOSEF (Korea Science and Engineering Foundation) and Myoungbo Dental Company under grant number 96-2-06-04-01-3. The authors wish to thank Dr Shiraishi, Dr Machuya and Dr Nakagawa of Kyushu University and Mr Uhm of Myoungbo Dental Company for helpful discussions.

References

1. R. M. GERMAN, *Inter. Met. Rev.* **27** (1982) 260.
2. E. RAUB and G. WORWAG, *Z. Metallkde.* **46** (1955) 52.
3. B. D. CULLITY, ''Elements of X-ray diffraction'', (Addison-Wesley, 2nd edn, 1978).
4. T. B. MASSALSKI, ''Binary alloy phase diagrams'', (ASM International, 1990).
5. P. ADEVA, G. CARUANA, M. ABALLE and M. TORRALBA, *Mater. Sci. Eng.* **54** (1982) 229.
6. S. BHAN and K. SCHUBERT, *J. Less-Comm. Metals* **17** (1969) 73.
7. B. COLES, *J. Inst. Metals* **84** (1956) 346.
8. I. KAWASHIMA, Y. ARAKI and H. OHNO, *J. Mater. Sci.* **26** (1991) 1113.

Received 21 August 1998
and accepted 29 April 1999